



Studying Thermal and Dynamical Stability of Interacting Rényi and Tsallis Holographic Dark Energy Models in LTB Inhomogeneous Universe

Mohamed Abdelrahmied¹, Ayman Aly², and Mustafa Selim¹

¹ Physics Department, Faculty of Science, Damietta University, New Damietta, Egypt; mohamed.a.elrashied@gmail.com

² Physics Department, Faculty of Science, Damanhour University, Damanhour, Egypt

Received 2024 August 27; revised 2024 December 12; accepted 2024 December 20; published 2025 February 3

Abstract

This work aims to investigate the different stability conditions of two scenarios of the inhomogeneous Lemaitre–Tolman–Bondi model of the universe with holographic dark energy. We considered the Rényi and Tsallis holographic models of interacting dark energy. These holographic models are investigated using the IR cutoff that equals the Hubble horizon. Various stability conditions of these models have been investigated to understand how much these models can tell us about the recent and future epochs of the universe in comparison with the cosmological constant model, or Λ CDM model. The conditions of violating the cosmological energy conditions have been studied. The evolution of the entropy and its first and second derivatives have been calculated and plotted for these holographic models. This gives an idea of how far these models satisfy the generalized second law of thermodynamics and hence have thermodynamical stability. The dynamical stability is studied for these evolved models, which give us glimpses of the dynamical stability at different phases of its evolution. We focus on investigating the stability in recent and near future times up to $z \leq -4$. Further investigation of stability has been obtained by studying the evolved sound speed squared parameter for these models, which gave us a final and decisive evaluation of the stability of these models.

Key words: (cosmology:) cosmological parameters – (cosmology:) dark energy – (cosmology:) large-scale structure of universe – cosmology: theory

1. Introduction

The accelerated expansion of the observable universe has been confirmed over the last decades. This observation has been confirmed using the observational data of distant supernovae (Riess et al. 1998; Perlmutter et al. 1999) and the cosmic microwave background (CMB, Ade et al. 2000; Huang et al. 2006). These observations also provided significant evidence for the existence of a cosmic component called dark energy (DE) which is thought to be responsible for the accelerated expansion of the observable universe. This component represents around 70% of the matter-energy content of the universe. Many measurements indicate that the cosmological constant model, the Λ CDM model, is very consistent with the observations. The Λ CDM model is based on the homogeneous and isotropic solution of Einstein field equations of general relativity, which is called the Friedmann–Lemaitre–Robertson–Walker (FLRW) metric. However, this scenario has some difficulties. The first is the cosmological constant problem in which the magnitude of the expected vacuum energy, calculated according to quantum mechanics, is very large (about 120 orders of magnitude different from the observed value). Second is the coincidence problem, where the DE density, ρ_D , is not only small but also in the same order of magnitude as matter density, ρ_m .

So, some cosmologists started to look for alternative models of the observable universe to explain its accelerated expansion. Some of these alternatives are the scalar field models such as Quintessence and K-essence. Other models include modified gravity models, higher-derivative gravity, etc. All these propositions are still open topics of research. Another alternative proposes that the universe is isotropic but inhomogeneous, rather than homogeneous as in the standard cosmological models. This inhomogeneous model is considered to explain the accelerated expansion of the universe without assuming the existence of the DE component. The most common one of these inhomogeneous models is the Lemaitre–Tolman–Bondi (LTB) model. This is based on the idea that we are living close to the center of a huge spherically symmetric matter underdensity with volume on the scale of Gigaparsecs (Gpc). This idea faced some difficulties as it is very unlikely that such underdense matter would be observed in any consistent large-scale cosmological observations. Instead, inhomogeneity can be assumed in the DE sector to explain the accelerated expansion without totally giving up the existence of DE (Grande & Perivolaropoulos 2011). This scenario considers the global structure of the universe as made of regions of matter whose matter density is less than its surroundings. These regions of matter underdensity are called voids or bubbles. In each of these bubbles, DE is assumed to have a constant density, as is

assumed in the Λ CDM model. Adopting this scenario has some observational consequences and this is useful in understanding some large-scale observations that are related to the existence of a preferred cosmological direction and cannot be explained consistently using the FRW universe with perfect fluids of cosmological constant DE and dark matter. These observations are: (i) planarity and the alignment of the CMB multipole moments, (ii) Large-scale alignment of the optical polarization data, (iii) Large-scale velocity bulk flow, (iv) Profiles of cluster halos. The inhomogeneous LTB model can predict that there is arbitrariness in the location of the observers near the center of the assumed isotropic inhomogeneity. This means that any off-center observer will naturally observe a preferred direction of an alignment of the low CMB multipole moments and bulk velocity flows.

Some of these observational phenomena can be explained by using an appropriate model of interacting DE with dark matter. It has been shown before by Sheykh (2011), Jahromi et al. (2018) that using the holographic dark energy (HDE) model with the Hubble horizon can explain the present state of the universe with consideration of the interacting DE scenario. This motivated us to use the HDE models with the Hubble horizon as the infrared (IR) cutoff to alternate the cosmological constant DE inside the proposed bubble of matter underdensity. The holographic model is mainly proposed to describe the physics of black holes and the evolution of its event horizons by connecting its three-dimensional bulk interior with its two-dimensional surface. This was first proposed by Hooft (1993) to give a prime description of a quantum theory of gravity inspired by black hole thermodynamics. It is later developed by Susskind (1995), Thorn (1994) to give a string theoretical description of this principle. It has been used in cosmology to describe the evolution of some cosmological models that can be considered as alternatives of the Λ CDM model. Recently, the HDE models became a very active topic of research in cosmology. In the interacting scenario of DE with cold dark matter (CDM), the evolution of the universe becomes non-adiabatic. This more generalized cosmological situation needs a generalized statistical formalism of the holographic principle entropy assigned to the horizon entropy of this interacting scenario of dark sectors. Recently, it has been proved that Rényi and Tsallis generalized entropies generate suitable models for the current universe. This motivated us to adopt these formalisms to analyze our scenario of the HDE. Many studies proposed a correspondence between thermodynamics and gravity, so generalizing one of the entropy or gravity concepts, as the black hole event horizon entropy idea, will change the other one. In previous work (Abd Elrashid et al. 2019; Aly et al. 2020) the non-interacting ordinary holographic model and Tsallis holographic dark energy (THDE) model have been considered with the LTB inhomogeneous DE universe. The evolution of some cosmological parameters against redshift was acceptable in comparison to some of the

Type Ia supernova observational data and was comparable with some other models of DE (Li et al. 2012; Jawad et al. 2018; Aditya et al. 2019). The THDE model has been investigated with many other cosmological models and the results compared with the predictions of the Λ CDM model and with various types of observations. Rényi holographic dark energy (RHDE) model is also studied with many cosmological scenarios. For example, the RHDE model has been explored with IR cutoff as the future and particle event horizons (Davis et al. 2003). The spatially homogeneous and anisotropic Bianchi VI_0 universe filled with RHDE with Granda-Oliveros and Hubble horizons as the IR cutoff have also been studied in the context of general relativity (Shekh 2023). It has been investigated with some other cosmological models (Komatsu 2017; Moradpour et al. 2018, 2017; Chunlen & Rangdee 2020) and the results are compared with the predictions of the Λ CDM model and with the observations. In another work under progress, we study the interacting RHDE model of DE to describe the evolution of the inhomogeneous LTB model, derive its cosmological parameters and check its viability to explain the recent observations. In this work we go further in studying the interacting RHDE model in the LTB universe. The various features and conditions of stability have been investigated. The same analysis of stability is done for the interacting THDE model in the LTB universe. The results of both models are compared continuously. In Section 2 we present the basic equations which represent the interacting RHDE and THDE models in the LTB universe. Specific LTB models have been chosen and their free parameters are specified based on our previous work on the same models in Aly et al. (2020), Abd Elrashid et al. (2019). In Section 3 the four energy conditions are investigated for both holographic models. The violation of these energy conditions in recent and near future times is analyzed and plotted against the redshift. The physical meanings of these results are also discussed.

In Section 4, the thermodynamic stability of these models is analyzed by studying the evolution of the entropy function and its first and second derivatives against the redshift. In Section 5, the dynamical stability of these models is discussed by defining the critical points of the evolution of these models at different time epochs. The phase space portrait is figured for these models and its dynamical behavior around the critical points and stability are discussed in detail. In Section 6, the evolution of the sound speed squared parameter is studied to obtain further investigation of the stability of these holographic models in recent and near future times. In the last section, some concluding remarks are given.

2. Basic Equations

We consider the interacting scenario between the considered HDE and CDM. Thus the energy conservation equation is

given by (Jawad et al. 2018)

$$\dot{\rho}_m + 3H\rho_m = -Q, \quad (1)$$

and

$$\dot{\rho}_D + 3H(\rho_D + P_D) = Q, \quad (2)$$

where Q is the interaction term which represents the coupling between dark sectors. If Q is positive this means the energy transfers from the dark matter sector to the DE sector while it means the opposite if Q is negative. The evolution of the cosmological models including the interaction of the dark sector has been extensively studied for different HDE models (Som & Sil 2014; Nayak 2020; Landim 2022; Saha et al. 2023; Rodriguez-Benites et al. 2024). Many estimations are considered for the interaction term of the dark sector. We will adopt here a simple interaction function that can be given by

$$Q = 3H\xi\rho_D, \quad (3)$$

where ξ is the coupling parameter of the interaction. The late-time constraints on interacting DE that were investigated in Benisty et al. (2024) revealed that the accepted values of ξ lay in $\xi \in [-0.33, 1]$.

2.1. Interacting Rényi Holographic Dark Energy in the LTB Universe

The quantum aspects of gravity motivated generalized definitions of entropy. These generalized definitions introduced some new concepts to the entropy such as non-additivity and non-extensivity. Rényi entropy is among those generalized entropy measures that was investigated widely in different cosmological setups and led to acceptable results. We consider the interacting RHDE model in the case of the LTB inhomogeneous universe and are interested in studying its stability conditions. The Rényi entropy is given by

$$S = \frac{1}{\delta} \ln \sum_{i=1}^n P_i^{1-\delta}, \quad (4)$$

where δ is the non-additivity parameter. The RHDE density is given by

$$\rho_D = \frac{3c^2H^2}{8\pi(1 + \frac{\delta\pi}{H^2})}, \quad (5)$$

where c^2 is a dimensionless constant and the IR cutoff is considered to be reciprocal of the Hubble Horizon, $1/H$. The energy conservation expressions, Equations (1) and (2), for the interacting HDE can be written for the LTB models as (Grande & Perivolaropoulos 2011)

$$\dot{\rho}_m + 2H\left(1 - \frac{P_t}{P_r}\right)\rho_m = -Q, \quad (6)$$

$$\dot{\rho}_D + 2H\left(1 - \frac{P_t}{P_r}\right)\rho_D = Q, \quad (7)$$

where P_t and P_r are the transverse and the radial components of the DE pressure respectively in the case of the LTB inhomogeneous universe. From Equations (3), (5), and (7) we can get

$$\left(\frac{P_t}{P_r} - 1\right) = \frac{3}{2}\xi + \frac{\dot{H}}{H^2}\left[2 - \delta + \frac{\delta\pi}{H^2 + \delta\pi}\right]. \quad (8)$$

Using Equation (11) in Grande & Perivolaropoulos (2011) $(\frac{P_t}{P_r} - 1)$ can be expressed as

$$\left(\frac{P_t}{P_r} - 1\right) = \frac{\dot{H}}{H^2} + \frac{3}{2} \frac{\lambda^3\Omega_m}{\lambda^3\Omega_m + \Omega_D}. \quad (9)$$

Substituting (9) in (8), we can write $\frac{\dot{H}}{H^2}$ as

$$\frac{\dot{H}}{H^2} = \frac{3}{2} \left[\frac{\xi - \frac{\lambda^3(1 - \Omega_D)}{\lambda^3(1 - \Omega_D) + \Omega D}}{\delta - 1 - \frac{\delta\pi}{H^2 + \delta\pi}} \right], \quad (10)$$

where $\lambda = \frac{R_0}{R}$, $R = R(r, t)$ is a function of space and time which plays the same role as the scale factor of the FRLW model of an isotropic and homogeneous universe and $R_0 = R(r, 0)$. The time derivative of Equation (5) for the HDE density gives

$$\dot{\rho}_D = \frac{2\dot{H}}{H} \left[2 - \delta + \frac{\delta\pi}{H^2 + \delta\pi} \right] \rho_D. \quad (11)$$

Combining this equation with $\dot{\Omega}_D = d\Omega_D/d \ln R = \dot{\Omega}_D/H$ we get

$$\dot{\Omega}_D = \left[-2\delta + 4 - \frac{-2H^2}{H^2 + \delta\pi} \right] \frac{\dot{H}}{H^2} \Omega_D, \quad (12)$$

which can be combined with Equation (5) to get

$$\Omega' = -3 \left(\xi - \frac{\lambda^3(1 - \Omega_D)}{\lambda^3(1 - \Omega_D) + \Omega D} \right) \Omega_D. \quad (13)$$

2.2. Interacting Tsallis Holographic Dark Energy in the LTB Universe

Another statistical generalization of the holographic entropy in which we are interested is the THDE. This model has been studied for specific LTB models by Abd Elrashied et al. (2019) where acceptable results obtained for some cosmological parameters are found to be comparable with some of the late universe observations. In this work we are interested in studying the stability conditions of the interacting THDE model in the LTB universe and comparing its stability features with those of the RHDE model. To do that we have to derive an evolution equation for the interacting Tsallis fractional DE density similar to Equation (13). We can start with the THDE density which is given by

$$\rho_D = BH^{-2\delta+4}, \quad (14)$$

where B is a parameter which can be written as $B = 3c^2 m_P^2 H^{2\delta-2}$, and m_P is the Planck mass. Now we can write

$$\left(\frac{P_t}{P_r} - 1\right) = \frac{3}{2}\xi + \frac{\dot{H}}{H^2}[2 - \delta]. \quad (15)$$

By combining this equation with Equation (9) we can write

$$\frac{\dot{H}}{H^2} = \frac{3}{2(\delta - 1)} \left(\xi - \frac{\lambda^3(1 - \Omega_D)}{\lambda^3(1 - \Omega_D) + \Omega D} \right). \quad (16)$$

By taking the derivative of Equation (14) we can write

$$\Omega' = (4 - 2\delta) \frac{\dot{H}}{H^2} \Omega_D. \quad (17)$$

From Equations (16) and (17) we can write

$$\Omega' = 3 \frac{\delta - 2}{\delta - 1} \left(\xi - \frac{\lambda^3(1 - \Omega_D)}{\lambda^3(1 - \Omega_D) + \Omega D} \right) \Omega_D. \quad (18)$$

2.3. Models of the Scale Function Ratio λ

In this work we consider the same LTB models that have been studied in Abd Elrashid et al. (2019) and Aly et al. (2020) which are given by choosing the scale function $R(r, t)$. Since our main interest is in the case of the on-center observer, i.e., the observer who is arbitrarily close to the center of the assumed void region with DE overdense in the LTB universe as proposed in Grande & Perivolaropoulos (2011), the scale function can only be chosen as follows

$$R(r, t) = (t + \beta + \eta_0 r^q)^{2/3}. \quad (19)$$

The range of values of the parameters is given as $\beta \in [0.5, 4]$, $q = 0.65$, and $\eta_0 = 50$ (Ribeiro 2008; Wang et al. 2000). The general formula of Hubble parameter as a function of the distance r from the center of the DE overdensity and time t for the inhomogeneous LTB universe is given by (Enqvist 2008; Aly et al. 2020)

$$H(r, t) = H_0 \sqrt{\lambda^3 \Omega_m + \Omega_D}, \quad (20)$$

where $H_0 = H(r, 0)$ and it can be expressed as a function of Ω_D as

$$H_0(r) = -2 \frac{(\ln[\sqrt{1 - \Omega_D} \sqrt{\Omega_D}] - \ln[\Omega_D + \sqrt{\Omega_D}])}{3t_0 \sqrt{\Omega_D}}. \quad (21)$$

3. Energy Conditions

Energy conditions have a crucial role in explaining many aspects of the universe such as its accelerated expansion and the occurrence of singularities in the cosmological models. Energy conditions are used to indicate the stability of the model over different cosmological phases and it is vital in the derivation of the black hole laws of thermodynamics. Energy conditions state the fact that the energy density in a specific

region of the universe should be positive and in general expressing the limitation of the energy-momentum tensor $T_{\mu\nu}$.

3.1. Strong Energy Condition SEC

The SEC can be expressed as $(T_{\mu\nu} - \frac{1}{2}Tg_{\mu\nu})u^\mu u^\nu \geq 0$ for all time-like four vectors u^μ . For the perfect fluid, it can relate the fluid density and its pressure as

$$\rho + 3P \geq 0. \quad (22)$$

The SEC is satisfied for matter and radiation in every phase of the universe. However, it is violated for DE because its anti-gravity property gives it negative pressure which does not satisfy this energy condition. This implies that the SEC has to be violated in the late accelerated of the universe. SEC is violated in other scenarios as well, and cosmological inflation is one among them.

3.2. Weak Energy Condition WEC

This condition is a mathematical expression of the fact that the observed matter-energy density should be positive when measured by any observer. This condition states that the energy-momentum tensor obeys the inequality $T_{\mu\nu}u^\mu u^\nu \geq 0$ which is simply written as

$$\rho \geq 0. \quad (23)$$

This condition is thought to be satisfied by all cosmic components at any phase of the evolution of the universe. It can be observed that both the RHDE and THDE models satisfy this condition at $\delta = \{3.5, 4.5, 5.5\}$ in the LTB universe as shown in Figures 1 and 2 respectively.

3.3. Dominant Energy Condition DEC

The DEC energy condition can be expressed as the inequality $T_{\mu\nu}u^\mu u^\nu \geq 0$. It is also stated that $T_{\mu\nu}u^\mu$ is always a non-spacelike vector. So, the DEC condition guarantees that the energy density is positive and the causality is satisfied as the energy density cannot flow in spacetime with a speed faster than the speed of light (Hawking & Ellis 2023). The DEC can be expressed for the perfect fluid case as

$$\rho - |P| \geq 0. \quad (24)$$

Although the DEC is satisfied by the standard cosmological model Λ CDM, it is found to be violated at the present time in the two cases of the interacting RHDE and THDE in the inhomogeneous LTB universe, as shown in Figure 3 for $\delta = 4.5$. It is interesting to note that the two holographic models have the same evolutionary behavior with z for all the chosen values of the δ parameter. In the near cosmic future, the DEC will be also violated for the two holographic models, however, at $z \leq -0.3$, DEC is satisfied by the interacting THDE model in the case of $\xi = -0.209$ where the energy is flowing from the DE sector to the dark matter sector.

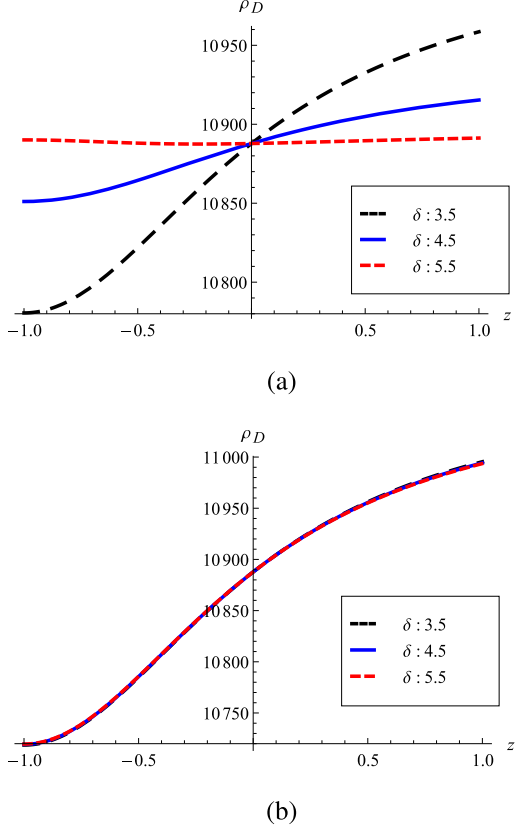


Figure 1. The evolution of the DE density of the RHDE model with z for (a) $\xi = -0.209$ and (b) $\xi = 0.290$.

3.4. Null Energy Condition NEC

NEC has a crucial role since its violation means the violation of WEC and SEC. This condition is vital in deriving the black hole laws of thermodynamics. This condition is stated as $T_{\mu\nu}k^\mu k^\nu \geq 0$ for every null vector k^μ and for the perfect fluid case it can be expressed as

$$\rho + P \geq 0. \quad (25)$$

To check the NEC for both holographic models, the evolution of $\rho + P$ with redshift is plotted in Figure 4. It can be observed that the NEC is violated by the two interacting cases of the RHDE model. In the case of the interacting THDE model, the NEC is violated for $\xi = 0.290$ while at $z \leq -0.3$, it is satisfied when $\xi = -0.209$. This leads to the SEC being violated for both holographic interacting models in recent times and the near future since the inequality (Equation (22)) is also violated as shown in Figure 5. Further, we can observe that the WEC is violated within the same range of cosmic time and redshift for the RHDE model because of the violation of the inequality (Equation (25)) as shown in Figures 1 and 2. The WEC is still violated for the interacting THDE model except at $z \leq -0.3$ for the case of $\xi = -0.209$ where it would be satisfied.

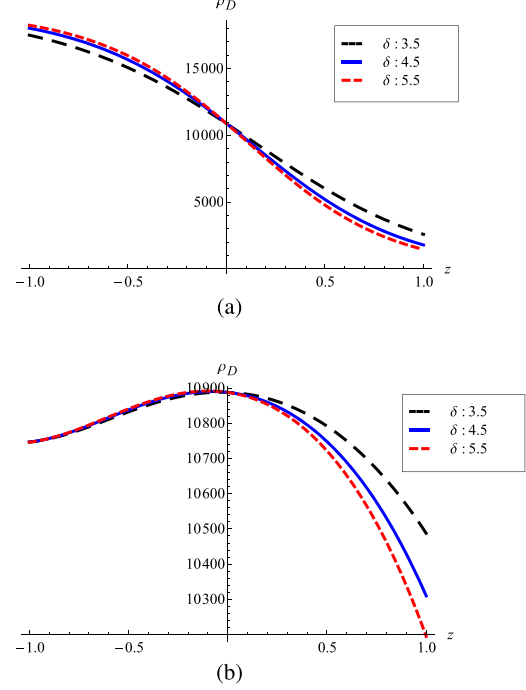


Figure 2. The evolution of the DE density of the THDE model with z for (a) $\xi = -0.209$ and (b) $\xi = 0.290$.

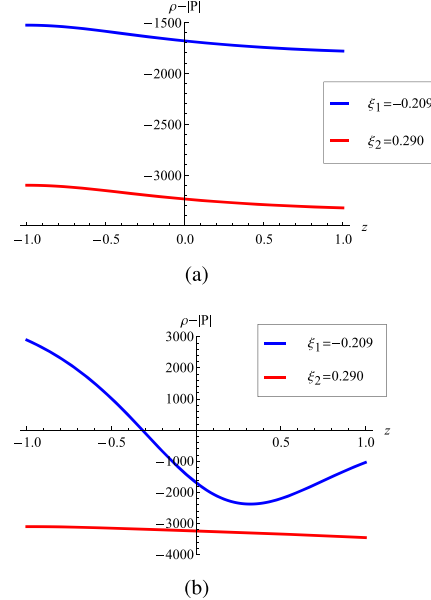


Figure 3. Violation of the DEC for (a) interacting RHDE model and (b) interacting THDE model in the inhomogeneous LTB universe at $\delta = 4.5$.

This violation of the NEC implies phantom-like behavior of these interacting HDE models in the LTB inhomogeneous universe. This behavior manifests itself again in the other perspectives of analyzing the stability that is studied later in

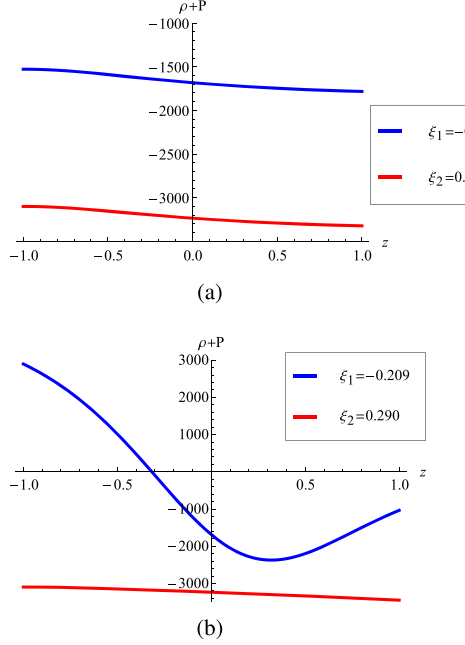


Figure 4. The evolution of $\rho + P$ with the redshift for (a) interacting RHDE model and (b) interacting THDE model in the inhomogeneous LTB universe at $\delta = 4.5$.

this work where the equation of state (EoS) parameter and the sound speed squared parameters have negative values in the present cosmic times and the near future.

4. Thermodynamics of RHDE and THDE Models

In this section, the thermal evolution of the holographic models in the LTB inhomogeneous case is analyzed. This is done by considering the generalized second law of thermodynamics, analyzing the evolution of the horizon entropy of the models, and investigating its maximization in the near cosmic future times.

4.1. Entropy

The second law of thermodynamics states that the entropy of any closed system should always increase. This should also be true for the systems with cosmological scales and the whole universe. Any system that has evolved boundaries has the entropy of its boundaries added to the entropy of its contents. The Hubble horizon is thought to be the thermodynamical boundary of the observable universe (Davis et al. 2003; John et al. 2023). So, the total entropy of the observable universe can be considered as the summation of its horizon entropy S_H and the entropy of its matter and energy content S_m . The generalized second law of thermodynamics can be written as

$$\frac{d}{dt}(S_m + S_H) \geq 0. \quad (26)$$

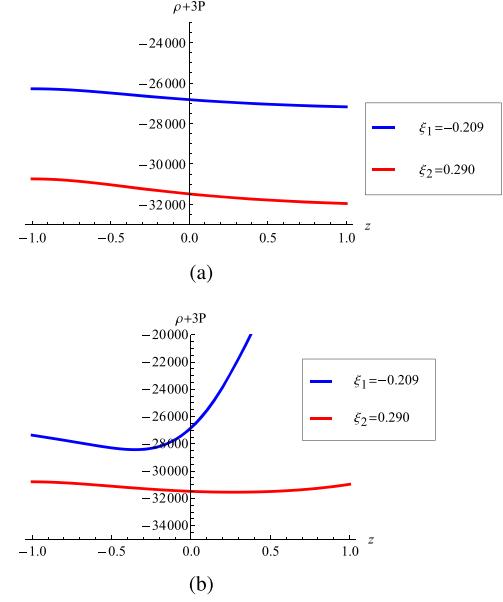


Figure 5. The evolution of $\rho + 3P$ with the redshift for (a) interacting RHDE model and (b) interacting THDE model in the inhomogeneous LTB universe at $\delta = 4.5$.

Since the horizon entropy is several orders of magnitude larger than the matter entropy, the total entropy can be approximated as the horizon entropy (Egan & Lineweaver 2010). The cosmological horizon entropy is given in a similar form as the black hole event horizon entropy which is defined by the Bekenstein law as (Bekenstein 1973)

$$S_H = \frac{A_H k_B}{4l_P^2}, \quad (27)$$

where $A_H = 4r_H^2$ is the horizon surface area, k_B is Boltzmann constant and l_P is the Planck length. For the observable universe which is locally flat, the horizon radius is $r_H = c/H$ and the horizon entropy is given by

$$S_H = \frac{\pi c^5 k_B}{\hbar G H^2}, \quad (28)$$

where \hbar is the reduced Planck constant and G is the gravitational constant. In natural units the horizon entropy can be simply expressed as

$$S_H = \frac{1}{H^2}. \quad (29)$$

By substituting the Hubble parameter given in Equation (20), the evolution of the horizon entropy, and hence the total entropy, with the redshift for the two holographic models can be studied. The evolution of total entropy is plotted for the two holographic

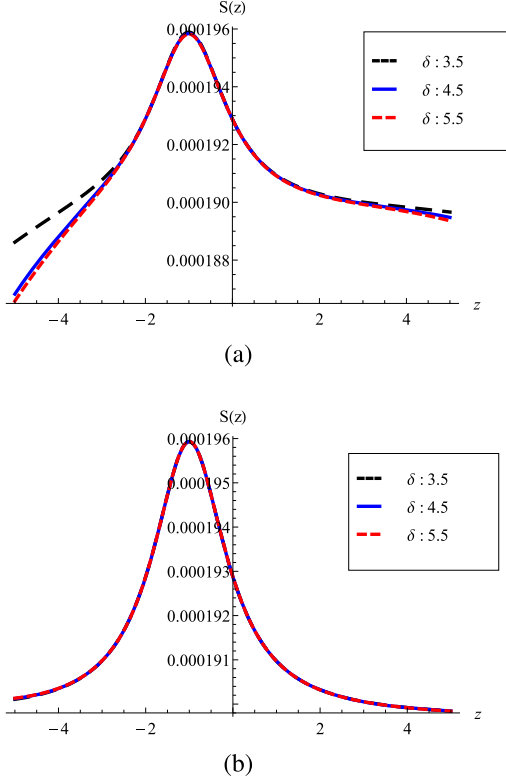


Figure 6. The evolution of the cosmological total entropy of the interacting RHDE model for the interacting case: (a) $\xi = -0.209$ and (b) $\xi = 0.290$.

models in Figures 6 and 7. In Figure 6 the cosmological entropy of the RHDE model increases with time in such a way that satisfies the generalized second law of thermodynamics. However, in the future, it evolves until reaching a maximum value at z then it decreases with time and violates thermodynamics. In Figure 7 the entropy of the THDE model is increasing with the evolution of the universe. Although the THDE entropy will reach a maximum value at nearly $z = -1$, at later times it will increase again. This means that the THDE model will be thermodynamically more stable in the future. To understand further the thermodynamical stability of the two holographic models in the future, the first and second derivatives of the entropy with the scale factor have been investigated.

The first derivative shows the stationary points of entropy where it has a zero first derivative with any convenient cosmological variable or $S' = 0$. The second derivative investigates whether the entropy function has a convex point of maximization where the second derivative of the entropy satisfies $S'' \leq 0$. Any natural system should have this convexity in the long time range of evolution to eventually satisfy the second law of thermodynamics and be thermally stable. For example, the Λ CDM cosmological model is found to satisfy this condition at the end of its de Sitter time (Krishna & Mathew 2017). The entropy derivatives for the two holographic

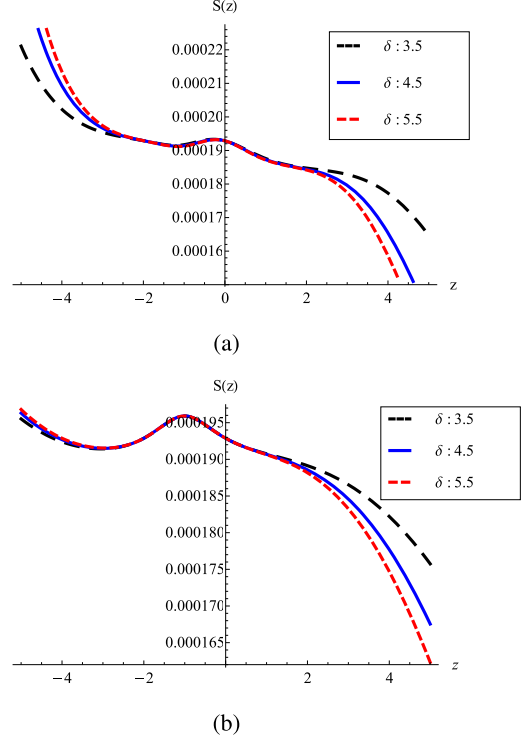


Figure 7. The evolution of the cosmological total entropy of the interacting THDE model for the interacting case: (a) $\xi = -0.209$ and (b) $\xi = 0.290$.

models are shown in Figures 8 and 9. In Figure 8(a) and (b), we can observe that for the RHDE model, the entropy has a stationary point in the future times at $z = -1$ for $\xi = -0.209$ and $\xi = 0.290$. This point corresponds to the maximum values of the entropy that are shown in Figure 7. At the later times of the far future at $z \leq -1$, the entropy first derivative has to be increasing then decreasing again until reaching zero. This means that after reaching its maximum value, entropy decreases again until vanishing. This behavior in the far future is showing itself again in investigating the evolutionary behavior of the entropy second derivatives, displayed in Figure 8(c) and (d) where the second derivatives will take positive values for $z \geq -2$ and hence there is no convexity of the entropy function in the far future. This violates the generalized second law of thermodynamics and shows the thermal instability of the RHDE model in the future times of the inhomogeneous LTB universe.

Figure 9 shows the stationary points of the THDE entropy function in plots in Figure 9(a) and (b) and the evolutionary behavior of its second derivatives in Figure 9(c) and (d). We can observe that entropy does not satisfy the convexity condition in the long run of evolution, i.e., far in the future, and hence does not satisfy the second law of thermodynamics. So, we can say in general that both HDE models have no bounded entropy and no ultimate thermal stability in the future.

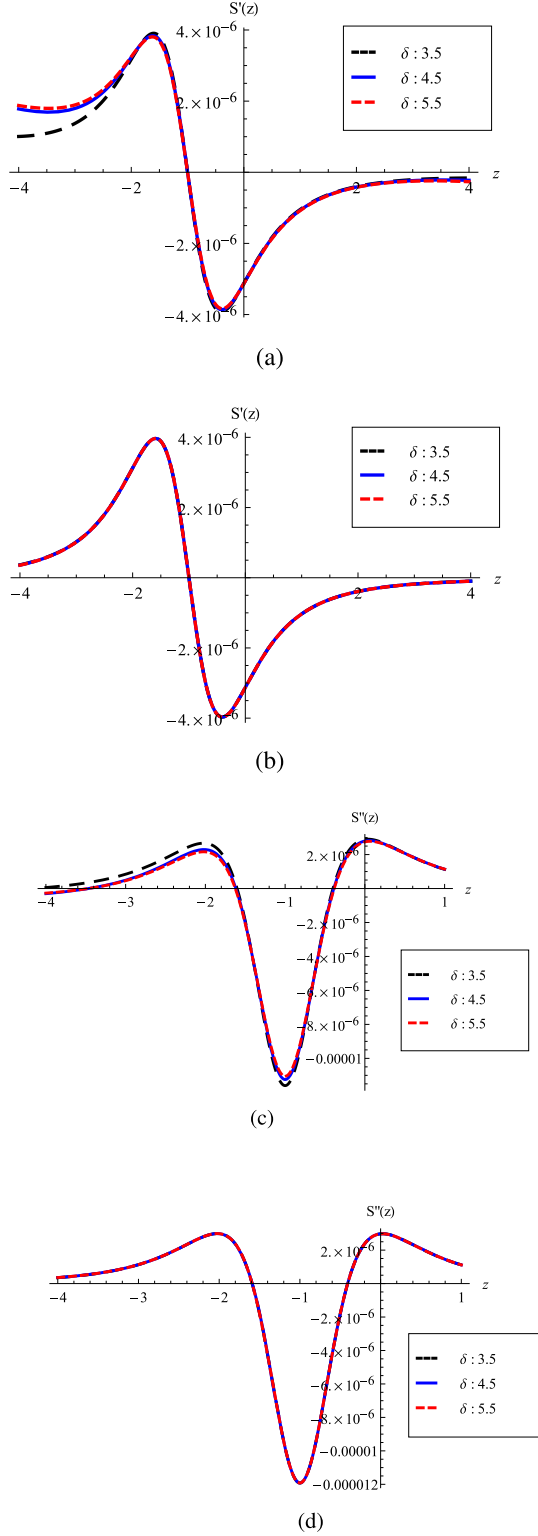


Figure 8. The evolution of the total entropy derivatives of the interacting RHDE model for $\xi = -0.209$ and $\xi = 0.290$.

This result is more consistent with that one obtained in the previous section about the phantom-like behavior of both models in the far future times. The thermal instabilities of these HDE models also may cause dynamic instabilities in the future evolution of the inhomogeneous LTB universe (John et al. 2023). This claim can be analyzed in more detail in the next section.

5. Dynamical Stability and Phase Space Analysis

The thermal analysis that has been discussed in the previous section reveals that the two interacting holographic models contradict the conventional thermodynamics in the long run of evolution with time. To investigate the reflections of this on the dynamical behavior of the LTB universe in the future, the evolution of some relevant dynamical variables could be done to understand exactly the behavior of the LTB universe in the asymptotic limits.

We can adopt the convenient choice of the dynamical variables given in Mathew et al. (2022) where

$$u = \frac{\rho_m}{3H^2}, \quad v = \frac{\rho_D}{3H^2}. \quad (30)$$

From Equation (20) of the Hubble parameter the two dynamical variables given above satisfy $u + v = 1$. By defining $x = \ln R(r, t)$, where $R(r, t) = (t + \beta + \eta_0 r^q)^{2/3}$, the conservation Equations (1) and (2) of the interacting HDE models with dark matter can be written as follows

$$\frac{d\rho_m}{dx} = -3\rho_m - \frac{Q}{H}, \quad (31)$$

$$\frac{d\rho_D}{dx} = -3(1 + \omega_D)\rho_D + \frac{Q}{H}. \quad (32)$$

Using these equations with Equation (3), the coupled differential equations for u and v can be written as,

$$\frac{du}{dx} = -3u - 3\xi v + 3u[u + (1 + \omega_D)v] = f(u, v), \quad (33)$$

$$\begin{aligned} \frac{dv}{dx} &= -3(1 + \omega_D)v + 3\xi u + 3v[u + (1 + \omega_D)v] \\ &= g(u, v). \end{aligned} \quad (34)$$

It is interesting to notice that these equations are always true for any interacting HDE model. Now, the task is to find the equilibrium (critical) points of these differential equations which can reveal the dynamical properties of the evolving LTB inhomogeneous universe with an interacting dark sector at different epochs of its history. These critical points are the key elements in constructing and analyzing the phase space of the relevant dynamical systems. The critical points are essentially obtained by setting $f(u, v) = 0$ and $g(u, v) = 0$. The resulting set of critical points is $(u_c, v_c) = \{(0, 0), (1, 0), (\frac{\xi}{\omega_D}, \frac{\omega_D - \xi}{\omega_D})\}$.

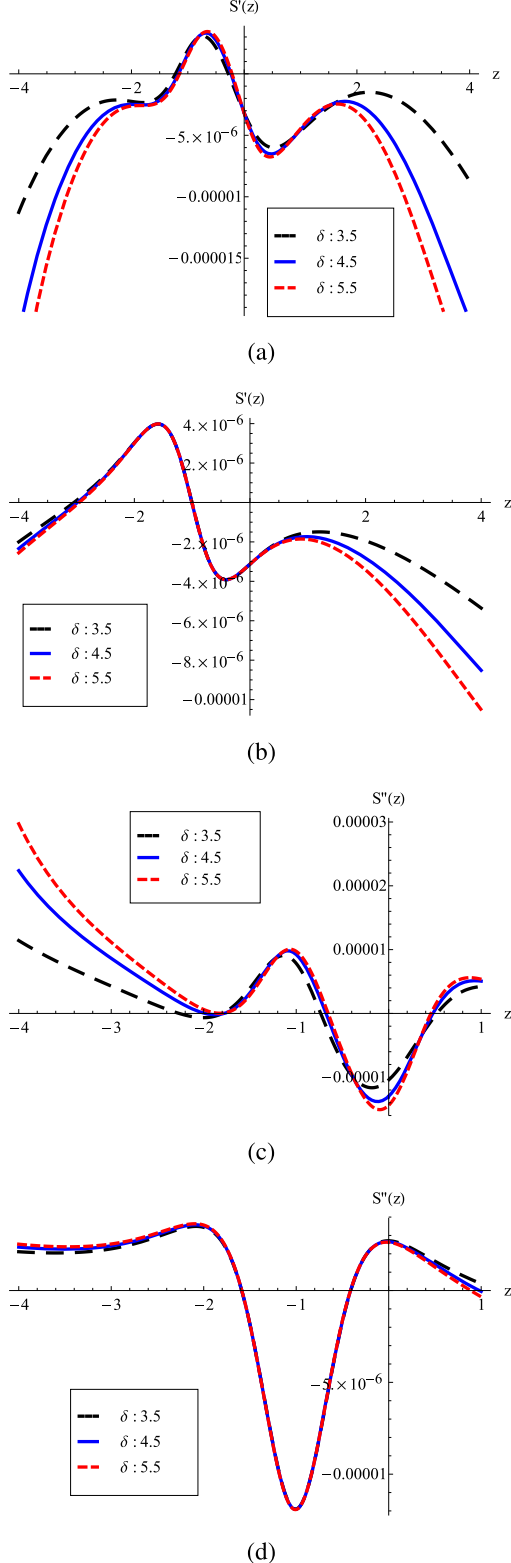


Figure 9. The evolution of the total entropy derivatives of the interacting THDE model for $\xi = -0.209$ and $\xi = 0.290$.

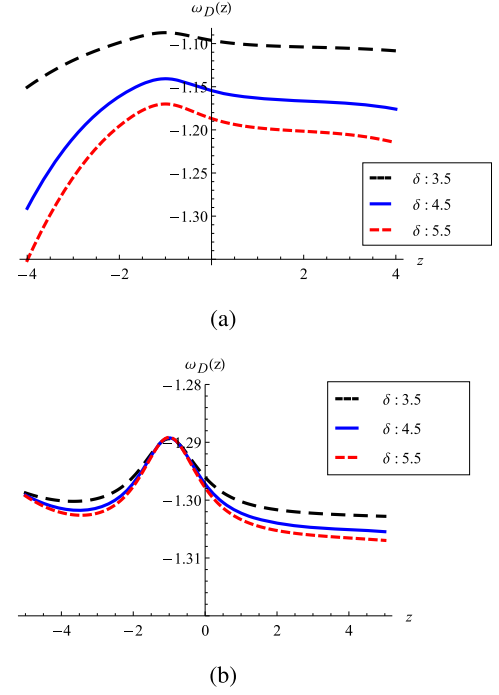


Figure 10. The evolution of the EoS parameter of the interacting RHDE model for $\xi = -0.209$ and $\xi = 0.290$.

The first point $(0, 0)$ is a trivial critical point which corresponds to an empty universe with no DE or dark matter. The second critical point $(1, 0)$ represents a matter dominated universe which is very close to the state of the very early universe. The third point $(\frac{\xi}{\omega_D}, \frac{\omega_D - \xi}{\omega_D})$ is the most relevant one. It can give us an understanding of the dynamical evolutionary behavior at any time epoch of the universe depending on the values of the parameter ξ and the EoS parameter of DE ω_D . This critical point is specifically useful in investigating the dynamical state of the universal system in the later times of the future (Usman & Jawad 2023). This is obvious when we consider the non-interacting holographic models, where $\xi = 0$. This point will become $(0, 1)$ which is the later de Sitter state of the DE dominated universe. The evolution of ω_D for both interacting holographic models is plotted against the redshift in Figures 10 and 11.

To study the stability behavior relevant to the last two critical points, the method of linear perturbation has to be considered. Here the dynamical variables are expressed around their critical values as $u \rightarrow u' = u_c + \delta u$ and $v \rightarrow v' = v_c + \delta v$, where δu and δv are the infinitesimal deviations of the dynamical variables from their critical values. By linearizing the coupled differential Equations (33) and (34) using this linear perturbation, one can obtain a matrix form for the perturbative

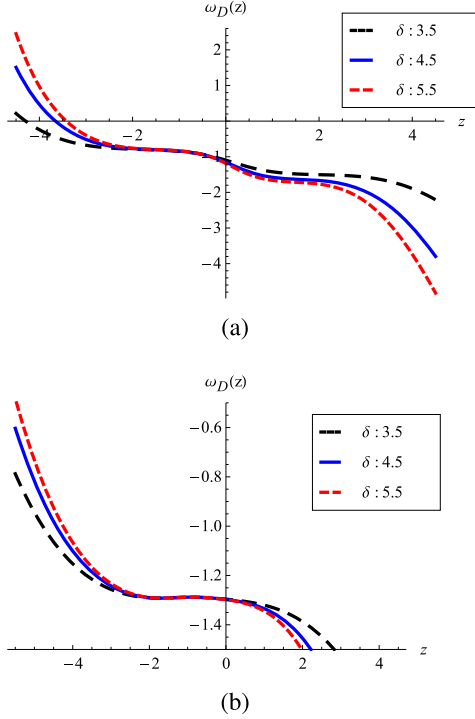


Figure 11. The evolution of the EoS parameter of the interacting THDE model for $\xi = -0.209$ and $\xi = 0.290$.

differential equations,

$$\begin{bmatrix} \delta u' \\ \delta v' \end{bmatrix} = \begin{bmatrix} \left(\frac{\partial f}{\partial u}\right)_c & \left(\frac{\partial f}{\partial v}\right)_c \\ \left(\frac{\partial g}{\partial u}\right)_c & \left(\frac{\partial g}{\partial v}\right)_c \end{bmatrix} \begin{bmatrix} \delta u \\ \delta v \end{bmatrix}. \quad (35)$$

The 2×2 Jacobian matrix on the right-hand side is given for the interacting holographic models by,

$$\begin{bmatrix} -3 + 6u + 3(1 + \omega_D)v & -3\xi + 3(1 + \omega_D)u \\ 3v & 3\xi + 3u + (1 + \omega_D)(6v - 3) \end{bmatrix}. \quad (36)$$

By diagonalizing this matrix we can find the two eigenvalues (λ_1, λ_2) corresponding to each critical point. Stability of the model is depending on the sign of its corresponding eigenvalues. If both eigenvalues are negative, the system is dynamically stable and the critical point represents a sink point to which the phase space trajectories converge. If both eigenvalues are positive, the critical point represents a source point in the phase space and the system is dynamically unstable. If one of the two eigenvalues is positive while the other one is negative, the critical point is a saddle point and the system will need further analysis to investigate its stability. To investigate the stability of the LTB universe with interacting RHDE and THDE models we have to find their eigenvalues

which correspond to the two nontrivial critical points of interacting systems.

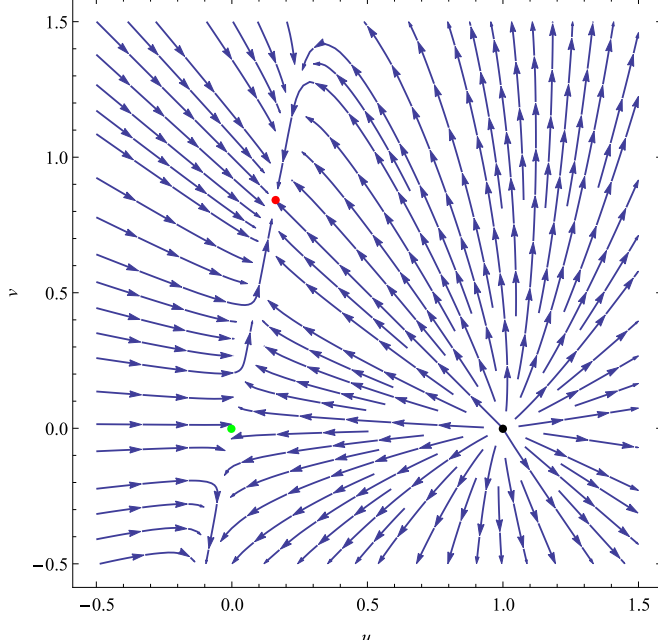
5.1. Dynamical Stability of RHDE Model

The first nontrivial critical point $(1, 0)$ has the eigenvalues $(3, 3(\xi - \omega_D))$. In the case of the RHDE model the EoS parameter ω_D is always negative in the range of redshift values illustrated in Figure 10. In the case of negative coupling constant $\xi = -0.209$ in Figure 10(a), the values of ω_D always satisfy the relation $|\omega_D| \geq 0.209$ and hence the corresponding eigenvalues are always positive. In the case of the positive coupling constant $\xi = 0.290$ in Figure 10(b), the eigenvalues are always positive for all the corresponding values of ω_D . So, we can say that the critical point $(1, 0)$ of the LTB universe with the RHDE model of DE represents a dynamically unstable point. This point is represented by the black dot in Figure 12 which is a source point from which all the phase space trajectories diverge. This is reasonable as this point represents the matter dominant state of the early universe which cannot be considered as a stable state of the observable universe.

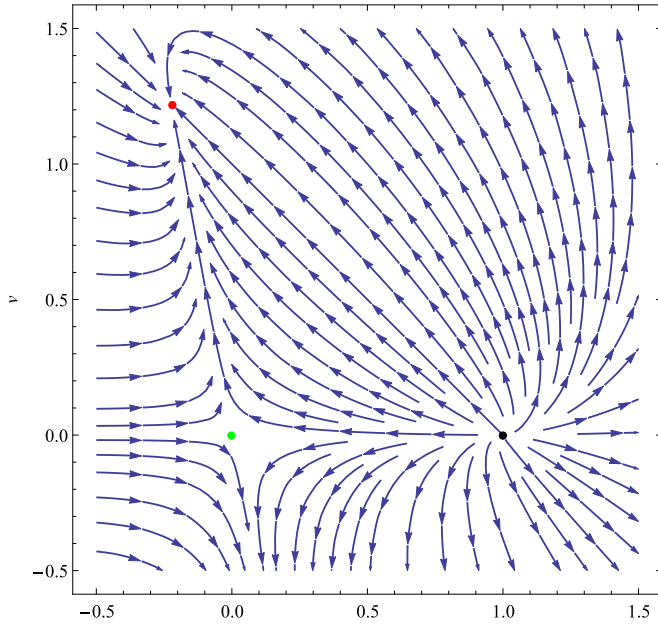
The second critical point $\left(\frac{\xi}{\omega_D}, \frac{\omega_D - \xi}{\omega_D}\right)$ has eigenvalues that can be analyzed using the Mathematical Wolfram program. These eigenvalues can be used to study the asymptotic dynamical behavior in the future times when the ω_D parameter has almost converged to the negative value -1.3 . In this case the critical point will degenerate to two critical points and there will be two sets of eigenvalues depending on the value of the coupling constant ξ . In the case of negative coupling constant $\xi = -0.209$, the critical point will be $(0.16, 0.84)$ which has the eigenvalues $(-0.79, 4.01)$. This is a saddle point in the phase space. In the case of positive coupling constant $\xi = 0.290$, the critical point will be $(-0.22, 1.22)$ which has the eigenvalues $(-0.57, 3.571)$. This is again a saddle point in the phase space. These saddle points are represented by the red dots in Figure 12. The phase space trajectories converge to a line passing these critical points. A stable critical point should have the phase space trajectories converge to that point but this feature is not strictly obeyed here. So, we cannot ensure that these critical points are stable points. However, in an infinitesimally small region around these points the phase space can be considered converging.

5.2. Dynamical Stability of THDE Model

The same analysis that has been done in the previous section can be repeated here with the LTB inhomogeneous universe with the interacting THDE model of DE. The evolution of ω_D parameter of the THDE model is shown in Figure 11. It can be noticed that the evolved ω_D will pass the value of $\omega_D = -1$ which is the de Sitter asymptotic state of the non-interacting holographic model and it is the same value as the one in the Λ CDM standard model of DE. So, we can investigate the



(a)

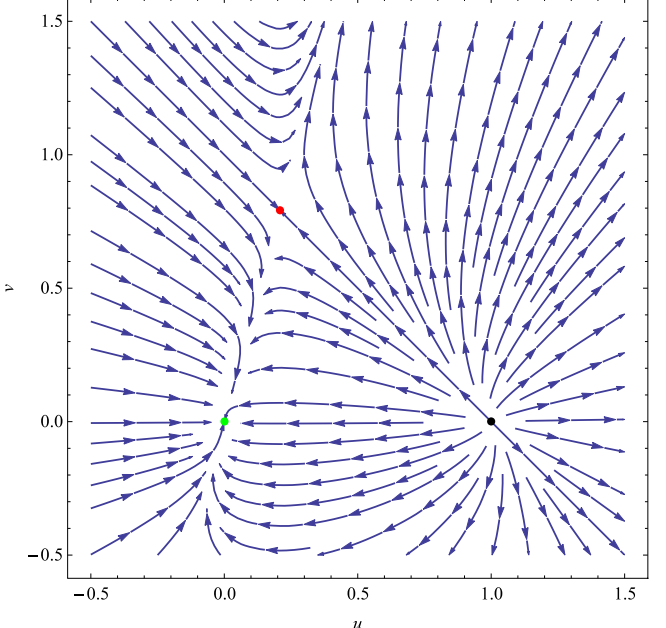


(b)

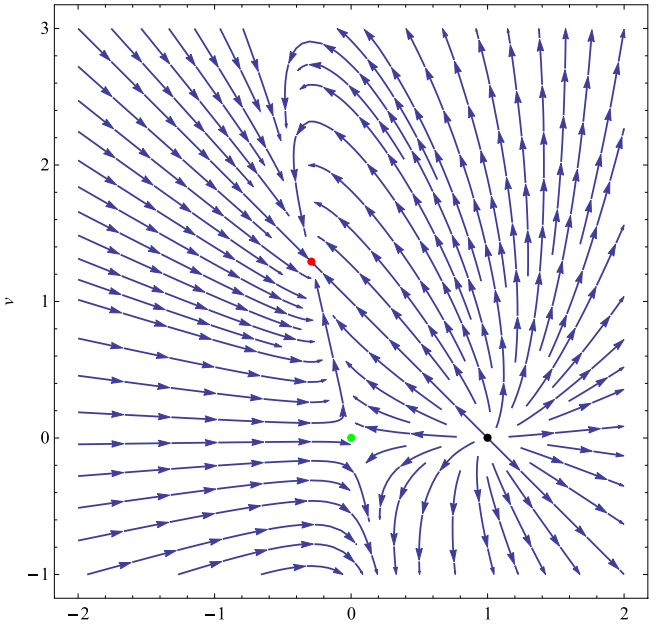
Figure 12. The phase space of the interacting RHDE model in the LTB universe for (a) $\xi = -0.209$ and (b) $\xi = 0.290$ where $\omega_D = -1.3$.

dynamical stability of the THDE model around that value in the future times.

The first critical point $(1, 0)$ can be investigated as we did before. It is noticed in Figure 11 that ω_D has negative values



(a)



(b)

Figure 13. The phase space of the interacting THDE model in the LTB universe for (a) $\xi = -0.209$ and (b) $\xi = 0.290$ where $\omega_D = -1$.

and satisfying $|\omega_D| \geq 0.209$ almost in the whole range of redshift of interest here. This again indicates an unstable matter dominated state of the LTB universe with the THDE model of DE. So, in Figure 13 the critical point $(1, 0)$ is represented by

the source point (black dot) in the phase space of THDE model from which all the phase trajectories are diverging.

The second critical point $(\frac{\xi}{\omega_D}, \frac{\omega_D - \xi}{\omega_D})$ can also be investigated as we did before. In the case of $\xi = -0.209$ the ω_D parameter is almost saturated at the value $\omega_D = -1$ in the future times, i.e., $z \geq -2$. In this case the critical point will be $(0.26, 0.74)$ and has the eigenvalues $(-0.43, 3.43)$ which mean that the critical point is a saddle point. In Figure 13(a) we can observe that the phase space trajectories locally diverge in an infinitesimal region around the critical point $(0.26, 0.74)$ which is represented by a red dot. However, this in general does not a guarantee that this point is unstable but at least locally it seems to be a point of dynamical instability.

In the case of the positive coupling constant $\xi = 0.290$ we notice that the evolved ω_D converges to $\omega_D = -1$ at a later time when $z \approx -4$. In this case the critical point will be $(0.29, 1.29)$ and has complex eigenvalues $(1.5 + 1.06i, 1.5 - 1.06i)$. Because the two eigenvalues are complex conjugates and have equal positive real parts, the phase portrait of the phase space trajectories around the critical point will be a growing spiral that rotates counterclockwise as shown in Figure 13(b). So, this model of the LTB universe will pass the point ω_D then it will leave it very rapidly to less negative values of ω_D . This indicates that this state is not dynamically stable.

The explicit dynamical instability of the LTB universe with the THDE model in future times seems very reasonable and predictive. This result is very consistent with that obtained in the previous section in which the model did not have a bounded entropy and was not thermodynamically stable. This is also agrees with the result obtained in Section 3 in that this model will converge to be phantom like and violate the all energy conditions.

However, this is not the case with the scenario of the LTB universe with RHDE model of DE. The dynamical stability analysis of this scenario shows that it is at least locally stable. So, we have the situation that the critical point $(\frac{\xi}{\omega_D}, \frac{\omega_D - \xi}{\omega_D})$ is dynamically stable at least locally but it is thermodynamically unstable. To go further in the stability analysis trying to clarify this paradoxical situation with the RHDE in the LTB universe, we can investigate the evolutionary behavior of the sound speed squared parameter in the next section.

6. Sound Speed Squared Parameter

The stability of the cosmological models can be investigated by studying the evolutionary behavior of the sound speed squared parameter V^2 . The real sound speed applies to the regular mode of propagation for density perturbations in the cosmic fluid and hence the stability of that system. The imaginary sound speed applies to the irregular mode of density perturbation propagation and hence classical instability. The physical values of V^2 have to be between 0 and 1. Any values out this range will indicate a tachyonic instability or

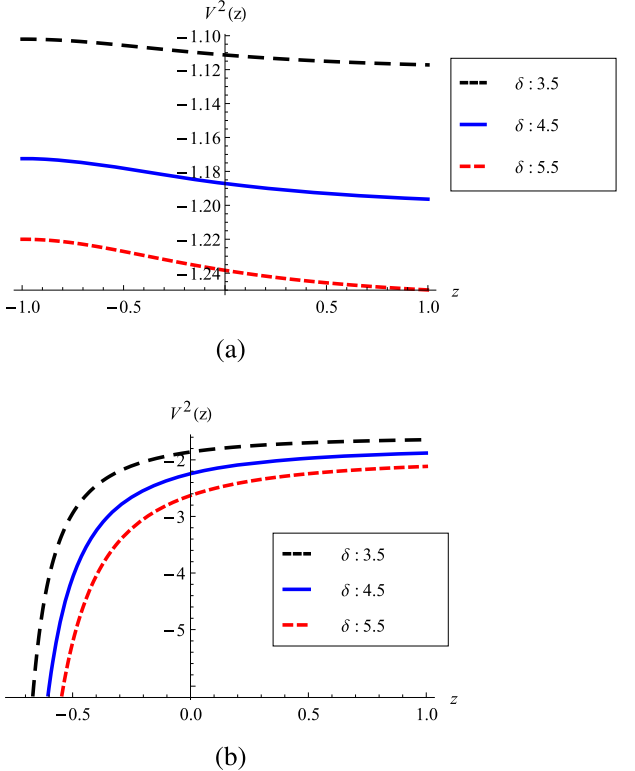


Figure 14. The evolution of sound speed squared of the interacting RHDE model in the LTB universe for (a) $\xi = -0.209$ and (b) $\xi = 0.290$ where $\omega_D = -1$.

superluminal propagation instability (Vagnozzi et al. 2020). The sound speed squared parameter is given by

$$V^2 = \frac{dP_D}{d\rho_D} = \frac{\rho_D \omega_D}{\dot{\rho}_D} + \omega_D, \quad (37)$$

where $P_D = \rho_D \omega_D$ is the DE pressure. Using ρ_D from Equations (5) and (14), the sound speed squared parameter is plotted for the two interacting holographic models in Figures 14 and 15.

As we can observe from these figures the V^2 parameter has only negative values in the recent and far future times of the universe. This means that these holographic models have instabilities in the perturbation level. They have irregular modes of superluminal propagation in which the density perturbations have an exponential growth (Myung 2007; Kim et al. 2008; Sharma & Dubey 2022).

This result is predictable for the THDE model since all previous methods of investigating stability have shown that this model is not stable in both recent and future times. However, in the previous section, when we analyzed the dynamical stability condition at the critical point $(\frac{\xi}{\omega_D}, \frac{\omega_D - \xi}{\omega_D})$, the model is found to be at least stable locally. However, its thermal stability analysis stated that it is unstable at the same time epochs. Now, by considering the last result derived from investigating the sound

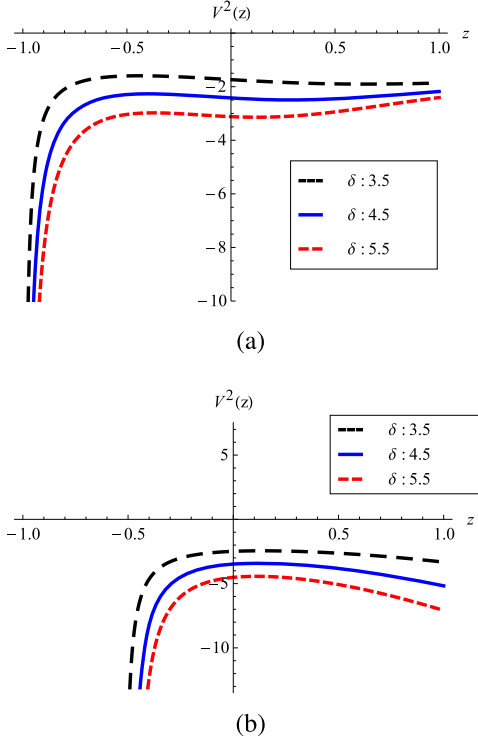


Figure 15. The evolution of sound speed squared of the interacting THDE model in the LTB universe for (a) $\xi = -0.209$ and (b) $\xi = 0.290$ where $\omega_D = -1$.

speed analysis for the RHDE model, we can conclude that this model of DE is also unstable whenever we consider the scenario of the LTB inhomogeneous universe.

7. Conclusion

In this work, we consider the interacting Rényi and Tsallis holographic models. These models are statistical generalizations of the entropy formula of a black hole which were introduced at first by Bekenstein and Hawking. These have been investigated in the case of the generalized LTB model of the inhomogeneous universe which was studied previously in Abd Elrashied et al. (2019), Aly et al. (2020), Grande & Perivolaropoulos (2011). The main target of our study is investigating the stability conditions of the inhomogeneous LTB universe in which a DE component is represented by the interacting RHDE and THDE holographic models. The significant interaction here is assumed to be between dark sectors only. We analyzed the stability of both models by examining their thermodynamic evolution and dynamical behavior in recent and future times.

In the beginning, we examined how well the gravitational energy conditions are satisfied, which have many applications in understanding gravitational and cosmological systems. We observed that both holographic models almost violate all

energy conditions. The violation of the SEC as shown in Figure 5 is a well-known theme of the systems containing DE because of its characteristic negative pressure. The violation of the NEC as shown in Figure 4 suggests that the DE density is evolving in such a way that makes these models unstable. The violation of the WEC refers to the phantom-like behavior (Pasqua et al. 2014) which is true as both models have almost negative values of the EoS parameter less than -1 as shown in Figures 10 and 11.

The analysis of thermodynamic stability had shown that both models are unstable in the far future, however, they seem stable in the near future. However, the THDE entropy is evolving in that it is always increasing with time as shown in Figure 7, and the entropy of the RHDE is increasing then rapidly decreasing at $z \approx -1$ as shown in Figure 6. So, the two models do not have a convexity condition in their entropy functions, i.e., $S'' \leq 0$, in the future for both values of the coupling constant ξ . However, both interacting holographic models have a temporary stability at the near future times, i.e., $S'' \geq 0$ at nearly $z \leq -1.5$ as shown in panels (c) and (d) of Figures 8 and 9. They eventually will lose this stability and their second derivative of entropy will turn to be positive in the later times.

The dynamical stability of both models has been investigated by analyzing the phase space and critical points for the two holographic models as shown in Figures 12 and 13. The analysis has affirmed that the THDE has an explicit dynamical instability at all of its critical points, while the RHDE model has a local stability at one critical point in its phase space. This motivated us to go further in the examination of stability and investigate the evolution of the sound squared parameter, V^2 , for both models. The later analysis revealed that the two holographic models have negative values of their evolving V^2 parameter as shown in Figures 14 and 15. This confirms the phantom-like behavior, and hence the instability of both holographic models in the recent and even near future times.

Accordingly, we can in general conclude that the LTB universe scenarios with interacting RHDE and THDE models of DE are not all promising. This is because of their explicit phantom-like behavior and their thermodynamic instability in the future which seems far from any promising candidate model that can explain the recent behavior of the universe and provide reasonable predictions about its future.

References

Abd Elrashied, M., Aly, A. A., & Selim, M. M. 2019, *JApA*, **40**, 15
 Ade, P., Balbi, A., Bock, J., et al. 2000, *ApJ*, **545**, L1
 Aditya, Y., Mandal, S., Sahoo, P., & Reddy, D. 2019, *EPJC*, **79**, 1020
 Aly, A. A., Elrashied, M. A., & Selim, M. M. 2020, *IJMPD*, **29**, 2050023
 Bekenstein, J. D. 1973, *PhRvD*, **7**, 2333
 Benisty, D., Pan, S., Staicova, D., Di Valentino, E., & Nunes, R. C. 2024, *A&A*, **688**, A156
 Chunlen, S., & Rangdee, P. 2020, arXiv:2008.13730
 Davis, T. M., Davies, P., & Lineweaver, C. H. 2003, *CQGra*, **20**, 2753
 Egan, C. A., & Lineweaver, C. H. 2010, *ApJ*, **710**, 1825
 Enqvist, K. 2008, *GReGr*, **40**, 451

Grande, J., & Perivolaropoulos, L. 2011, *PhRvD*, **84**, 023514

Hawking, S. W., & Ellis, G. F. 2023, The Large Scale Structure Of Space-time (Cambridge: Cambridge Univ. Press)

Hooft, G. 1993, arXiv:[gr-qc/9310026](https://arxiv.org/abs/gr-qc/9310026)

Huang, Z.-Y., Wang, B., Abdalla, E., & Su, R.-K. 2006, *JCAP*, **2006**, 013

Jahromi, A. S., Moosavi, S., Moradpour, H., et al. 2018, *PhLB*, **780**, 21

Jawad, A., Bamba, K., Younas, M., Qummer, S., & Rani, S. 2018, *Symm*, **10**, 635

John, R., Sarath, N., & Mathew, T. K. 2023, *EPJC*, **83**, 697

Kim, K. Y., Lee, H. W., & Myung, Y. S. 2008, *PhLB*, **660**, 118

Komatsu, N. 2017, *EPJC*, **77**, 229

Krishna, P., & Mathew, T. K. 2017, *PhRvD*, **96**, 063513

Landim, R. G. 2022, *PhRvD*, **106**, 043527

Li, X., Wang, S., Huang, Q., Zhang, X., & Li, M. 2012, *SCPMA*, **55**, 1330

Mathew, T. K., et al. 2022, arXiv:[2204.12097](https://arxiv.org/abs/2204.12097)

Moradpour, H., Bonilla, A., Abreu, E. M., & Neto, J. A. 2017, *PhRvD*, **96**, 123504

Moradpour, H., Moosavi, S., Lobo, I., et al. 2018, *EPJC*, **78**, 829

Myung, Y. S. 2007, *PhLB*, **652**, 223

Nayak, B. 2020, *GrCo*, **26**, 273

Pasqua, A., Chattopadhyay, S., Khurshudyan, M., & Aly, A. A. 2014, *IJTP*, **53**, 2988

Perlmutter, S., Aldering, G., Goldhaber, G., et al. 1999, *ApJ*, **517**, 565

Ribeiro, M. B. 2008, arXiv:[0807.0866](https://arxiv.org/abs/0807.0866)

Riess, A. G., Filippenko, A. V., Challis, P., et al. 1998, *AJ*, **116**, 1009

Rodríguez-Benites, C., González-Espinoza, M., Otalora, G., & Alva-Morales, M. 2024, *EPJC*, **84**, 276

Saha, A., Chanda, A., Dey, S., Ghose, S., & Paul, B. 2023, *MPLA*, **38**, 2350024

Sharma, U. K., & Dubey, V. C. 2022, *IJGMM*, **19**, 2250010

Shekh, S. 2023, *InJPh*, **97**, 983

Sheykhi, A. 2011, *PhRvD*, **84**, 107302

Som, S., & Sil, A. 2014, *Ap&SS*, **352**, 867

Susskind, L. 1995, *JMP*, **36**, 6377

Thorn, C. B. 1994, arXiv:[hep-th/9405069](https://arxiv.org/abs/hep-th/9405069)

Usman, M., & Jawad, A. 2023, *IJMPD*, **32**, 2350100

Vagozzi, S., Visinelli, L., Mena, O., & Mota, D. F. 2020, *MNRAS*, **493**, 1139

Wang, B., Abdalla, E., & Osada, T. 2000, *PhRvL*, **85**, 5507